Coastal Engineering 131 (2018) 31–41

Contents lists available at ScienceDirect

Coastal Engineering

journal homepage: www.elsevier.com/locate/coastaleng

Drivers of alongshore variable dune erosion during a storm event: Observations and modelling

Kristen D. Splinter *, Edward T. Kearney, Ian L. Turner

Water Research Laboratory, School of Civil and Environmental Engineering, UNSW Sydney, Sydney, Australia

ARTICLE INFO

Keywords:
Dune erosion
Narrabeen-Collaroy
Storm Impact Scale
Collision regime
Swash regime
Dune impact model

ABSTRACT

The ability to understand and predict alongshore-variable sand dune erosion is key to better coastal management. This study utilizes detailed observations (immediately pre, during and post-storm topography, waves and water levels) collected over a 6-day period at the 3.6 km long Narrabeen-Collaroy beach in south-east Australia, to identify and explore drivers of the highly variable alongshore dune erosion caused by an East Coast Low storm in June 2011. Key characteristics of the immediately pre-storm subaerial morphology obtained by airborne Lidar (beach slope, dune toe elevation, dune height) varied considerably alongshore. Daily airborne Lidar surveys conducted at low tide indicated considerable temporal variability in the evolution of the subaerial beach profile. Despite considerable alongshore variability in the magnitude of modelled inshore wave heights during the storm, it was instead observed that the predominant determinant of maximum dune erosion was the pre-storm dune toe elevation. A simple dune impact model forced with local alongshore-variable inshore wave modelling was found to successfully predict up to 85% of the observed alongshore variability in dune erosion at this site, with this erosion tidally modulated over the 6 days to time periods when the waves were directly impacting the dune. Importantly, alongshore variation in wave height is shown to account for just 10% of the alongshore variability in dune erosion during this storm. These results reconfirm that knowledge of the pre-storm subaerial morphology, in particular the elevation of the dune toe with respect to time-varying water levels during a storm, is a key driver of alongshore variability in the erosion response along dune-backed sandy coastlines.

1. Introduction

Along sandy coasts it is generally accepted that beaches will accrete during less energetic wave conditions, and erode during more energetic wave conditions (Aubrey, 1979; Wright and Short, 1984; Stive et al., 2002; Quartel et al., 2008). The most energetic wave conditions that occur in the coastal environment are coastal storms; events which can potentially cause considerable beach erosion and dominate the short-term erosion history of the coastline (Russell, 1993; Frazer et al., 2009). The risk posed by coastal erosion is recognised as considerable and potentially increasing as a result of elevated sea levels, changing regional weather patterns, and growing populations and infrastructure located in the coastal zone (IPCC et al., 2007; Callaghan et al., 2009; Ruggiero et al., 2013; Anderson et al., 2015; Barnard et al., 2015).

The destructive potential of storms due to large waves and/or elevated water levels is not a new phenomenon. For example, Australia's east coast was battered by a series of large storms in 1967 and then again by storms in 1974 (McGrath, 1968; Foster et al., 1975; McLean and Thom, 1975; Bryant and Kidd, 1975; Splinter et al., 2014). Most recently, an East Coast Low storm event in June 2016 stripped 11.5 M m^3 of subaerial sediment from 177 km of surveyed sandy coastline in New South Wales (Australia) (Harley et al., 2017). In the past decade devastating hurricanes have caused billions of dollars of damage and widespread erosion along the eastern USA (Stockdon et al., 2007; van Verseveld et al., 2015), while strong El-Nino/La Nina events are linked to large erosion on the west coast of the USA (Allan and Komar, 2006; Barnard et al., 2011) as well as more generally across the Pacific basin (Barnard et al., 2015). In the winter of 2013/2014 Europe was impacted by a series of large extra-tropical wave events that caused significant and widespread coastal erosion (Castelle et al., 2015; Masselink et al., 2016a, 2016b). Within these studies, it is frequently observed that there is considerable variability in storm-induced dune erosion in the alongshore direction at scales of 10s–1000s of meters, which may be due to the presence of offshore sand bars, localized rip currents, and alongshore gradients in wave height (Castelle et al., 2015; Loureiro et al., 2012; Coco et al., 2014; Senechal et al., 2015; Harley et al., 2015), as well as

* Corresponding author.
E-mail address: k.splinter@unsw.edu.au (K.D. Splinter).

https://doi.org/10.1016/j.coastaleng.2017.10.011
Received 12 December 2016; Received in revised form 6 August 2017; Accepted 29 October 2017
Available online 3 November 2017

morphological characteristics of the subaerial beach such as the elevation of the dune toe, dune height and beach slope (Overton and Fisher, 1988, 1994; Larson et al., 2004; Palmsten and Holman, 2012; Plant and Stockdon, 2012; Splinter and Palmsten, 2012; Palmsten et al., 2014; Palmsten and Splinter, 2016; Houser, 2013; Sallenger, 2000; Houser et al., 2008).

Previous studies that use numerical models to compute design coastal erosion volumes and engineering setbacks are typically hampered by a general lack of immediately pre- and post-storm beach profile data (Roelvink et al., 2009; Mariani et al., 2012; Ranasinghe et al., 2013). Roelvink et al. (2009). used predominantly laboratory scale experiments for the development of the 2DH process model XBEACH, whilst the field-scale dataset of storm erosion that was included had a 4-month lag between the available pre-storm survey and the onset of the storm event, introducing uncertainty regarding the true pre-storm condition of the beach. Similarly the study by McCall et al. (2010). utilised pre-storm data that preceded the storm event by 4 months. Due to lack of available data, Splinter and Palmsten (2012) were likewise limited to using pre-storm data that preceded the storm event by between 6 and 9 months. And again, Stockdon et al. (2007). estimated the impact of hurricane landfall using pre-storm survey data obtained 12 months prior. In all cases, the lack of immediate pre-storm data is implicitly brought into the calibration process via tuning of model free parameters, which inevitably can lead to highly storm- and/or site-specific calibration. In order to minimise errors in modelling and truly understand the drivers of the erosion response, the pre and post-storm surveys need to be as recent to an event as possible (Morton et al., 1993).

Here we present daily observations of alongshore-variable dune erosion obtained by rapid-response airborne Lidar deployed within a single 3.6 km long embayment during a 6-day storm wave event. Utilizing a simple model framework (Palmsten and Holman, 2012; Splinter and Palmsten, 2012), we explore the key drivers with respect to hydrodynamic (tides and runup) and morphological (beach slope and dune toe elevation) drivers that account for our observations. In the next section the study site and data (airborne Lidar surveys, waves and water levels) are described. This is followed by a presentation of the observed alongshore-variable erosion response in Section 3. A simple empirical dune erosion model is used to interpret the observed alongshore-variable response in Section 4, which is followed by a synthesis (Section 5) and summary of the key findings in Section 6.

2. Background

2.1. Study site

Narrabeen-Collaroy embayment is located approximately 20 km north of the city of Sydney on the southeast coastline of Australia (Fig. 1). The embayment is bounded to the south by the prominent Long Reef Point and at its northern end by Narrabeen Head. The enclosed sandy beach is 3.6 km in length and is composed of fine to medium quartz sand underlain by sandstone bedrock, with a median sand grain size $D_{50} \approx 0.3$ mm, exhibiting typical gradients for the nearshore and intertidal of 0.02 and 0.12 respectively. The site experiences a micro-tidal semi-diurnal tide with a mean spring tidal range of 1.6 m.

Due to the prevalence of moderate to high wave energy conditions and the exposed orientation of the central and northern end of the beach

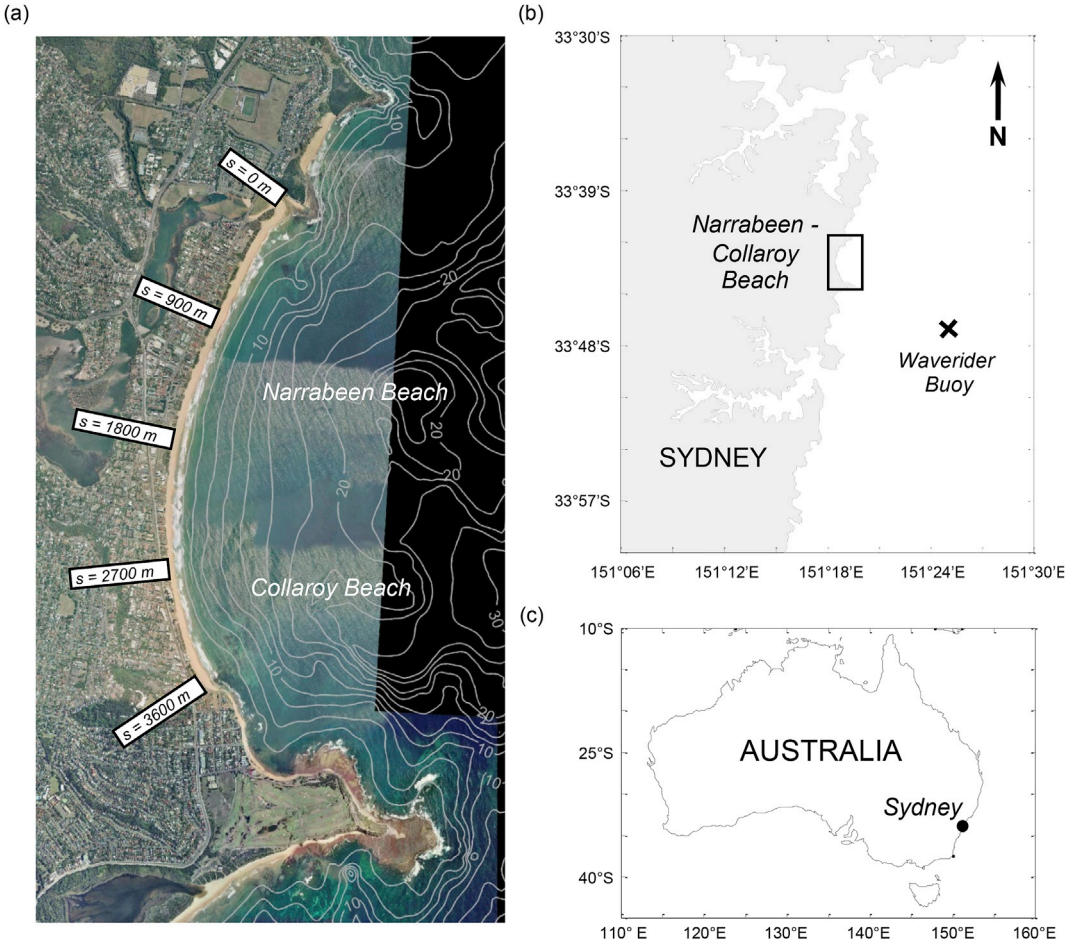

Fig. 1. (a) Map of the Narrabeen Embayment on the south east Australian coastline with superimposed log spiral alongshore positions as per Harley and Turner (Harley and Turner, 2008). (b) Regional map of Sydney with location of wave buoy. (c) Map of Australia with location of Sydney.

to the prevailing SSE swell waves, the morphodynamic response of Narrabeen-Collaroy Beach is highly alongshore variable and rapid. The beach is defined as an intermediate beach based on the Wright and Short (1984) classification, with the beach state predominantly influenced by episodic storm events whereby erosion and accretion can occur at any time of the year, with a lesser seasonal trend also observed (Harley et al., 2011; Davidson et al., 2013). The sandbar morphology is typically in the intermediate range and alternatives between alongshore uniform sandbars to low-tide terraces. A long-term and unbroken beach monitoring program has been active at Narrabeen-Collaroy since 1976 (Turner et al., 2016). These data include hourly ARGUS coastal imaging commencing in 2004 that span the southern half of the embayment, a continuous fixed profile scanning Lidar that has been operating since 2013, and on-demand UAV and airborne Lidar flights to capture immediate pre- and post-storm response.

2.2. June 2011 East Coast Low: wave and water level data

On June 13, 2011, meteorological forecasts indicated that an East Coast Low (ECL) was forming rapidly off the coast of south east Queensland and moving south, and predicted to generate storm waves in Sydney in excess of 5 m. Hourly wave data was recorded during the subsequent storm at the Sydney wave rider buoy located in 76 m water depth to the east of the Long Reef headland (Fig. 1). The deep water characteristics of this storm measured at Sydney are presented in Fig. 2. The storm had a duration of 39 h (defined as time when offshore $H_s > 3$ m), which is shorter than the average for Sydney of 64 h, although the peak of the storm ($H_s = 4.5$ m) was slightly above the average of 3.98 m (Shand et al., 2011). The peak spectral wave period of the storm ranged from 8 to 13 s and the direction of the waves varied throughout the storm as it passed southward, ranging from 120 to 180° TN (Fig. 2; middle panel). The astronomical tidal range (Fig. 2; bottom panel) at the time of the storm was 1.58 m (mean spring tidal range at Narrabeen is 1.6 m).

In order to capture the alongshore variability in the nearshore wave height at this distinctly curved embayment, a SWAN nearshore wave model (Booij et al., 1999) was used to transform the measured offshore waves in to the 20 m depth contour (refer Fig. 1a for the alongshore coordinate system at this site). To aid interpretation, in Fig. 3 the modelled output in the curved grid (Easting, Northing (*EN*)) obtained at 20 m × 20 m resolution was converted to a rectangular *xy* coordinate system based on a log-spiral transformation (Harley and Turner, 2008).

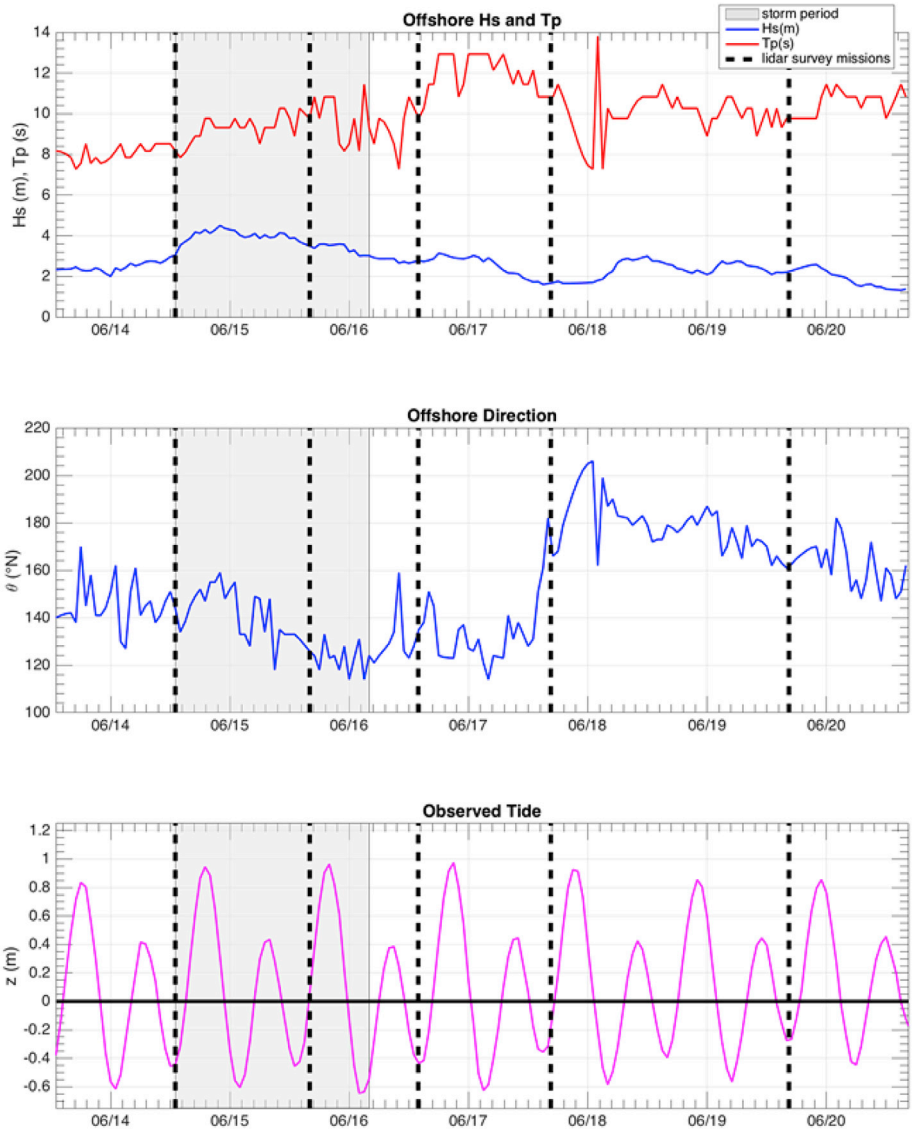

Fig. 2. Summary of offshore wave characteristics for the June 2011 East Coast Low storm event. (top) Offshore significant wave height and peak wave period. (middle) Offshore wave direction. (bottom) Observed water levels. Vertical dash lines represent the time of low-tide Lidar survey missions flown at Narrabeen during the storm.

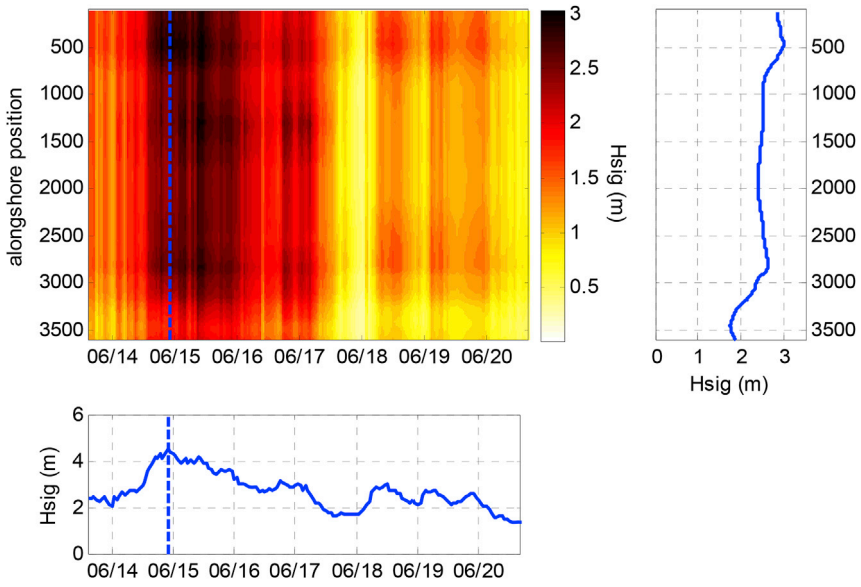

Fig. 3. Summary of modelled nearshore waves for June 2011 ECL storm using SWAN. The heat map (upper left panel) presents the modelled significant wave height across the embayment at a depth of 20 m as it evolves through time. The right panel shows the instantaneous significant wave height at the peak of the storm (indicated by the dotted line). The lower panel shows the offshore significant wave height through time for reference with the peak of the storm identified by the dashed line.

The top left panel illustrates how the nearshore significant wave height in 20 m depth varied alongshore during the 6-day storm event. The alongshore variability of the modelled significant wave height in 20 m at the peak of the storm is presented in the right panel and shows a general N-S trend of decreasing nearshore wave height.

2.3. Rapid response pre-, during and post-storm topographic data

To quantify the subaerial topography of the beach immediately before, during, and post-storm, a rapid response airborne Lidar method was employed. Previously reported analysis of this system shows that a vertical accuracy of 0.02 m can be achieved (Middleton et al., 2013). Horizontal resolution of the Lidar data used here was 0.25 m × 0.25 m.

Five low-tide surveys spanning a six-day time-window were flown to capture the immediate pre-storm topography and the progression of beach erosion during the storm, as well as the initial recovery. The timing of these surveys with respect to the storm are indicated in Fig. 2 (vertical dashed lines). For ease of analyses and interpretation, the curvilinear Lidar data was transformed to the local rectangular coordinate system (*xyz*) as described in Section 2.2. Cross-shore profiles every 10 m in the alongshore were extracted from the transformed Lidar data for further analysis.

The horizontal and vertical location of the dune toe at each 10 m alongshore-spaced cross-shore profile corresponding to each daily Lidar survey was defined as the furthest seaward local maxima of curvature of a smoothed cross-shore profile following the method of Stockdon et al. (2007). To be selected as a dune toe, the local maxima of curvature was required to be greater than a threshold of 0.025 based on sensitivity testing and visual verification. Utilization of a break in slope term to define the dune toe is commonly used (Plant and Stockdon, 2012; Splinter and Palmsten, 2012; Stockdon et al., 2009; Mull and Ruggiero, 2014; Serafin and Ruggiero, 2014; Pye and Blott, 2008) and preferred over more subjective approaches, such as the highest astronomical tide (Saye et al., 2005). The authors acknowledge that other methods of determining dune toe elevation, such as the vegetation line may be more appropriate on natural systems such as barrier islands where foredunes and incipient dunes are also present. Due to the nature of Narrabeen-Collaroy, a vegetation line is not a useful indicator of the dune toe. The beach slope, β, was computed as the linear best-fit gradient between the dune toe and the shoreline, defined here as the 0.7 m AHD (Australian Height Datum) contour (Stockdon et al., 2007). The volume of observed dune erosion was computed as the change in sand volume landwards of the pre-storm dune toe.

3. Observations

3.1. Alongshore-variable beach and dune erosion

The morphological response to the June 2011 East Coast Low (ECL) event was observed to be highly alongshore variable within the 3.6 km long Narrabeen-Collaroy embayment, with some areas of the subaerial beach exhibiting considerable erosion, while other areas remaining seemingly unaffected (Fig. 4). The central region of the beach between alongshore positions 1400 and 1800 m (refer Fig. 1a) exhibited considerable dune erosion, with the dune face receding up to 3 m landwards. Dune scarps of up to 3 m high were formed, with dune fencing and vegetation being undermined and collapsing onto the beach.

For this storm, across the entire embayment there were three main zones of morphodynamic behaviour based on total subaerial volume eroded. Zone 1 extended between 100 m and 900 m alongshore and showed alternating (order 100 m) beach face erosion and accretion similar in appearance to rhythmic bar beach and cusp morphology (Fig. 4). Within this zone an area of considerable subaerial erosion volume (~20 m^3/m) occurred at 190 m alongshore, which was primarily due to the removal of a terraced berm area near the shoreline, while the dune was unaffected. Zone 2 stretched from 900 m to 1800 m alongshore and also exhibited considerable subaerial erosion. Between 1400 m and 1800 m alongshore there were high levels of dune erosion. The third zone stretched from 1800 m to 3600 m alongshore and was characterised by alternating (order 200 m) regions of erosion and accretion at the beach face, with no changes in the dune.

Using the unique daily airborne Lidar surveys that are available during this storm, the temporal response at select profiles within each of these three zones (Fig. 5) highlights the alongshore variability in the observed storm erosion at this site. The upper left panel of Fig. 5 depicts the profile at 840 m alongshore position (Zone 1), and along with the lower right panel showing profile 3300 m alongshore (Zone 3), demonstrate profiles where there was little to no observed volume change and no dune erosion. In comparison, the upper right panel of Fig. 5 shows that the 1760 m profile (Zone 2) exhibited considerable erosion between June

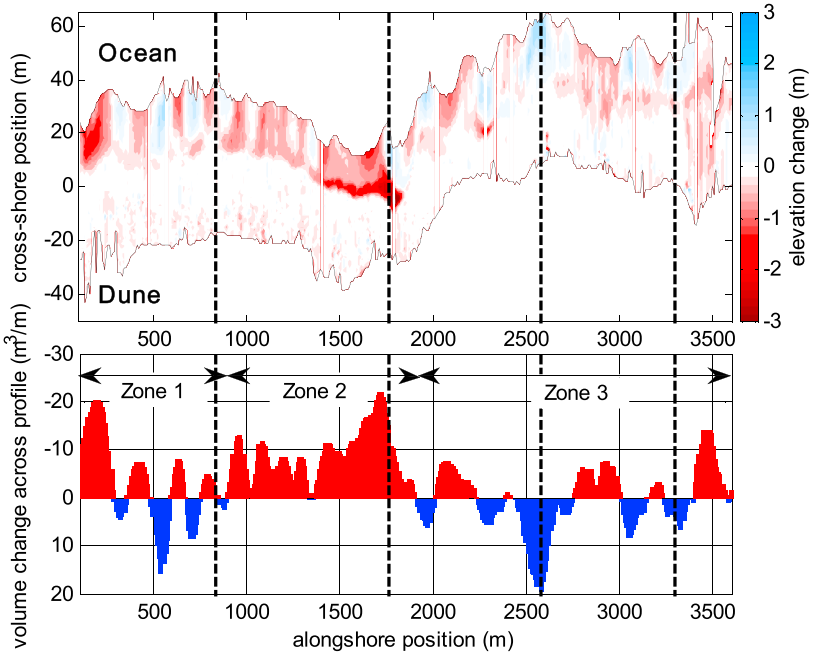

Fig. 4. Heat map of elevation change after the storm event (upper panel) and total amount of observed erosion above MSL at all locations alongshore (lower panel). The vertical dotted lines indicate profiles of interest detailed in Fig. 5.

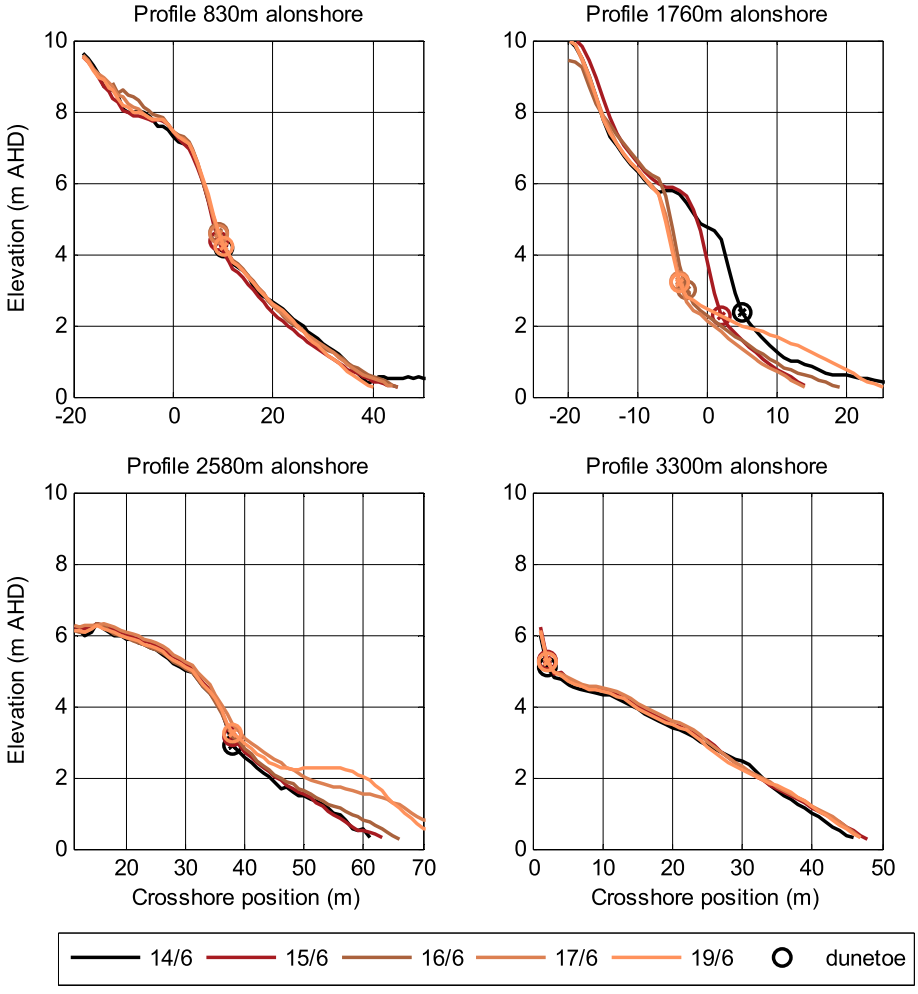

Fig. 5. Summary of characteristic morphological responses throughout the embayment in response to the June 2011 East Coast Low storm event.

14th and 16th that was followed by some recovery and accretion around the mean sea level (z = 0 m AHD) shoreline between June 17th and 19th. The lower left panel shows that the profile at 2580 m alongshore position (Zone 3) did not exhibit any significant erosion but there was a substantial volume of accretion about the MSL shoreline of approximately 20 m^3/m between June 16th and 19th. This highlights the considerable temporal and spatial variability in the erosion response along this single 3.6 km embayment for the June 2011 ECL.

3.2. Total water levels relative to dune toe elevation

To better understand the drivers of alongshore variable response of Narrabeen-Collaroy beach during the June 2011 ECL, particularly why some areas experienced considerable dune erosion while other areas experienced virtually none, Hourly total water levels were compared to the evolving dune toe elevation (z_{dt}) derived from the repeat airborne Lidar surveys. Total water levels (TWL) were estimated as the sum of the measured ocean water level plus 2% runup exceedance, the latter calculated by (Stockdon et al., 2006):

$$R_2 = 1.1\left(0.35\beta(H_0L_0)^{\frac{1}{2}} + \frac{\left[H_0L_0\left(0.563\beta^2 + 0.004\right)\right]^{\frac{1}{2}}}{2}\right) \quad (1)$$

where H_0 is the offshore significant wave height (m), L_0 is the offshore wavelength (m), and β is the foreshore beach slope. R_2 was computed hourly at each 10 m-spaced alongshore location using the modelled nearshore waves (Section 2.2) that were reverse shoaled using linear wave theory to their deep-water equivalent (H_o) and the daily Lidar-derived beach slope measured between the dune toe and the 0.7 m AHD contour (Section 2.3).

Fig. 6 shows the magnitude of the total water level at the peak of the storm relative to the pre-storm dune toe location (top panel), as well as the pre-storm beach slope (middle panel) and the observed dune erosion volume (bottom panel). The pre-storm beach slope (middle panel) depicts a steeper beach in the northern two-thirds of the beach between 100 m and 2700 m alongshore (peak at y = 1370 m), and a flatter beach in the southern third of the embayment, with an overall average slope of 0.12. The average measured pre-storm dune toe elevation was 4.08 m AHD, with a maximum dune toe elevation of 8.32 m (y = 410 m) and a minimum of 1.67 m (y = 2870 m), showing considerable alongshore variability in pre-storm morphology. The alongshore-average calculated total water level at the peak of the storm was 3.45 m AHD. There is a clear visual correspondence (Fig. 6 top and bottom) between areas of dune erosion and where the maximum total water level (TWL) exceeded the dune toe.

Fig. 7 and Fig. 8 illustrate the temporal variability of the calculated total water level relative to dune toe elevation and the measured profile evolution throughout the storm at contrasting alongshore locations 1760 m (Zone 2) and 830 m (Zone 1). At profile 1760 m (Fig. 7) where dune erosion was observed, the initial dune toe was at an elevation of 2.39 m AHD. There is a clear temporal dependence on erosion (Fig. 7 bottom), with erosion occurring between June 14th and 17th when water levels exceeded the measured dune toe. During the first 24 h of the storm, the dune first eroded back and the dune toe lowered in elevation. After the peak of the storm had passed, the dune toe eroded landwards and upwards (June 15–17). Between June 15–17, application of Sallenger's Storm Impact Scale (Sallenger, 2000) indicates a strong tidal

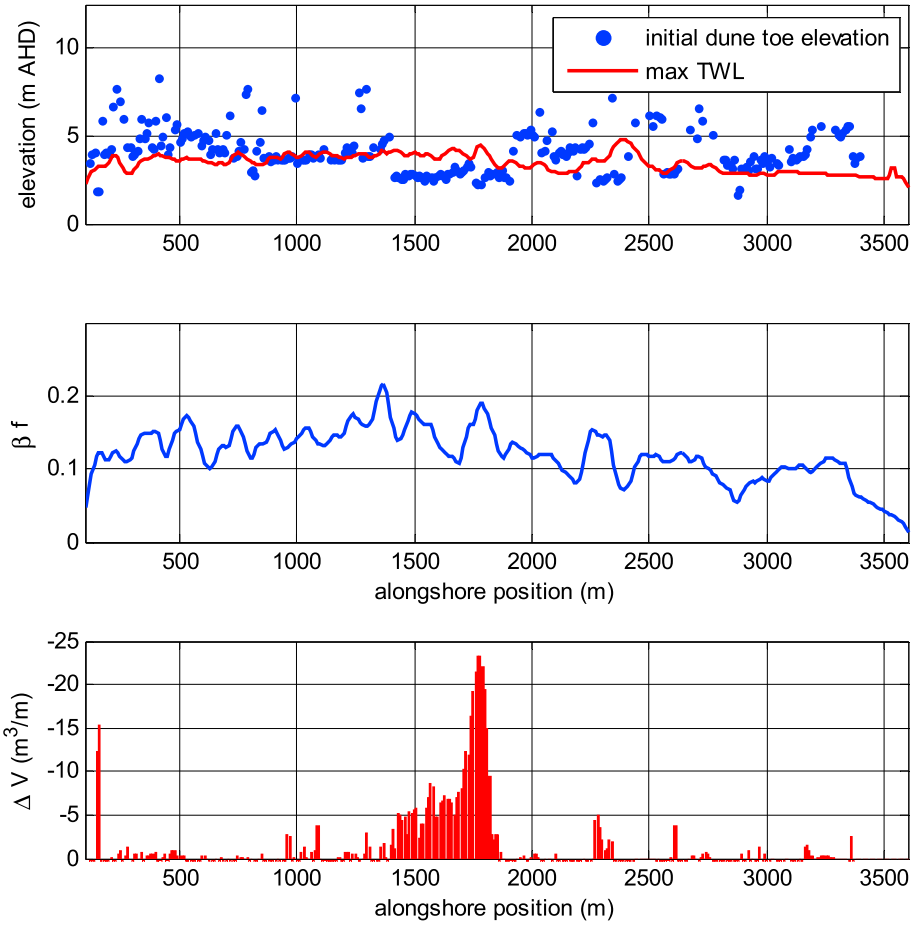

Fig. 6. Summary of dune toe and beach slope measurements. (upper panel) Plot of dune toe elevation compared to the modelled maximum total water level for reference. (middle panel) Beach slope at all locations along the embayment. (lower panel) Observed dune erosion volume over the duration of the storm.

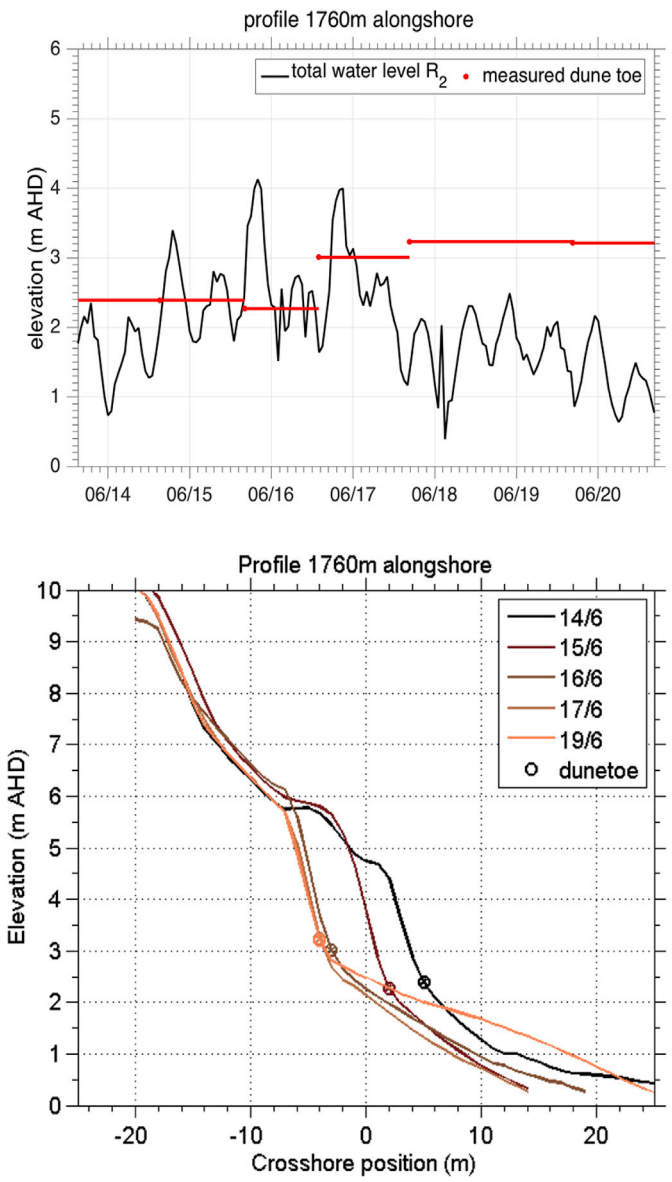

Fig. 7. (upper panel) Profile 1760 m total water level, dune toe elevation throughout the storm, and (lower panel) observed evolving profile through time.

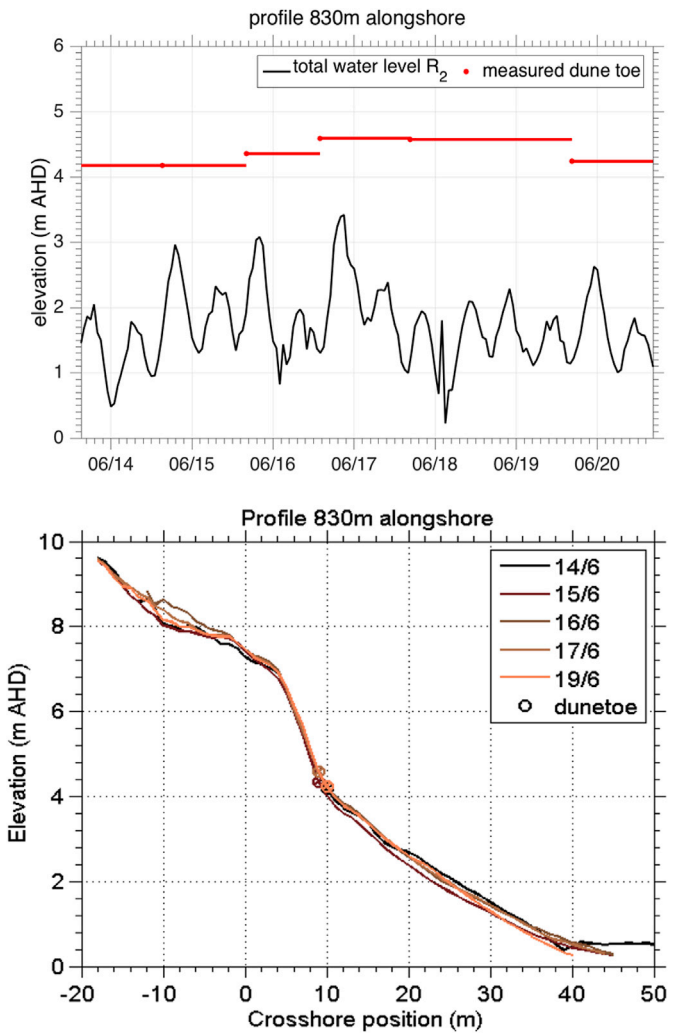

Fig. 8. (upper panel) Profile 830 m total water level, dune toe elevation throughout the storm, and (lower panel) observed evolving profile through time.

dependence, oscillating between the swash regime characterised by total water levels not exceeding the dune toe, and the collision regime where the TWL exceeded the elevation of the dune toe. After June 17th, total water levels receded and did not reach the elevated dune toe. During this time period after the peak of the storm had passed (June 18–19), the commencement of accretion was observed across the lower beach.

By comparison, the location at profile 830 m (Fig. 8) exhibited minimal observed beach change throughout the storm. Comparing the time-varying total water levels with measured dune toe elevations (Fig. 8 top panel) reveals that in this region of the embayment, the beach was always in a swash regime and total water levels never reached the elevation of the pre-storm dune toe at 4.18 m AHD. To examine this temporal and alongshore variability in observed erosion response in more detail, a calibrated dune impact model is now presented in the following section.

4. Predicting erosion volumes using a simple dune impact model

The ability to predict the spatial and temporal variability in subaerial erosion over large (alongshore) areas would be a valuable tool for the coastal engineer and manager. While there has been significant work undertaken on the development of complex process-based models such as XBEACH (Roelvink et al., 2009), these models are presently highly sensitive to a number of factors, including errors in the antecedent beach state and the choice of a specific subset of parameters used for calibration (Splinter and Palmsten, 2012; Mariani et al., 2012; Vousdoukas and Ferreira, 2012; Callaghan et al., 2013; Harley et al., 2016; Simmons et al., 2017). More simple empirical models that attempt to quantify the volume of sand eroded from a coastal dune during storm attack require less forcing data and have fewer parameters to be calibrated (Overton and Fisher, 1988, 1994; Larson et al., 2004; Palmsten and Holman, 2012). The observations presented in Figs. 7 and 8 suggest that simple erosion models based on a dune impact approach may be useful to predict the erosion potential of a storm at this site. Here, the simple empirical dune erosion model presented in Palmsten and Holman (2012) is used to further explore the temporal and alongshore-variable morphological response that was observed during the June 2011 ECL.

Erosion volume above the dune toe (ΔV) due to wave impact is predicted by:

$$\Delta V = 4C_s(R_2 - Z_{dt})^2 N_c \tag{2}$$

Where R_2 is given by eq. (2), Z_{dt} is the elevation of the dune toe, C_s is a calibration coefficient, and N_c quantifies the number of collisions of waves with the dune based on a probability distribution:

$$N_c = \left[P\left(Z_{R2} + Z_{tide} + Z_{surge} > Z_{dt}\right)\right] \cdot \frac{t}{T_p} \quad (3)$$

where $P(Z_{R2})$ is the normally distributed 2% exceedance runup elevation and Z_{tide} and Z_{surge} are the tide and surge elevations, t is the time of exposure and T_p is the peak wave period. When the calibrated model was tested on field data at the Gold Coast, Australia, errors in dune retreat were less than 13% (Splinter and Palmsten, 2012).

To test the model's ability to predict dune erosion, two approaches were explored: the first allowed dune toe, slope, and profiles to be updated based on each daily Lidar-derived low-tide profile. The second approach assumed only a pre-storm beach profile was available. For both approaches, a single value for the calibration coefficient C_s was calculated across the entire 3.6 km embayment by means of linear regression such that the squared difference between the observed and modelled erosion volumes were minimised.

Along the entire 3.6 km embayment, the calibrated model ($C_s = 1.27 \times 10^{-3}$) was able to reproduce 59% of the observed variability in the dune erosion with a RMSE = 2.47 m^3/m, when using the daily evolving dune toe and beach slope data with the hourly nearshore wave data (Fig. 9 top). When tested using the pre-storm topographic survey only, the calibrated model ($C_s = 9.98 \times 10^{-4}$) explained 48% of the observed variability in dune erosion with a RMSE = 2.82 m^3/m. It is expected that a lower magnitude coefficient would be determined for the latter test as the initial dune toe was lower than if it was allowed to evolve landwards and upwards as was observed, thus reducing the exposure of the dune to subsequent wave impact as the storm progressed.

Overall, the simple wave impact dune erosion model was able to reproduce and highlighted the spatial and temporal variability of the observed erosion at Narrabeen-Collaroy for the June 2011 ECL.

5. Discussion

5.1. Morphological feedback

In a forecasting sense, where it always is the case that only pre-storm topography will be available, the simple dune impact approach explored in Section 4 showed reasonable skill ($R^2 = 0.48$) at predicting alongshore-variable dune erosion within the Narrabeen-Collaroy embayment, when only the pre-storm airborne Lidar data was used. Allowing for morphological feedback, by either updating the topography daily with new observations as was possible for this study, or developing a time-varying dune erosion model (Splinter and Palmsten, 2012), increases model skill. This is to be expected as the dune toe elevation and beach slope evolve throughout the duration of the storm as the profile erodes and moves towards equilibrium. For the specific observations presented here, where the dune was tidally impacted by wave runup, the dune toe was observed to predominately recede landward and upward (e.g. Fig. 5) as has been observed elsewhere for both laboratory and field investigations (Larson et al., 2004; Palmsten and Holman, 2012; Splinter

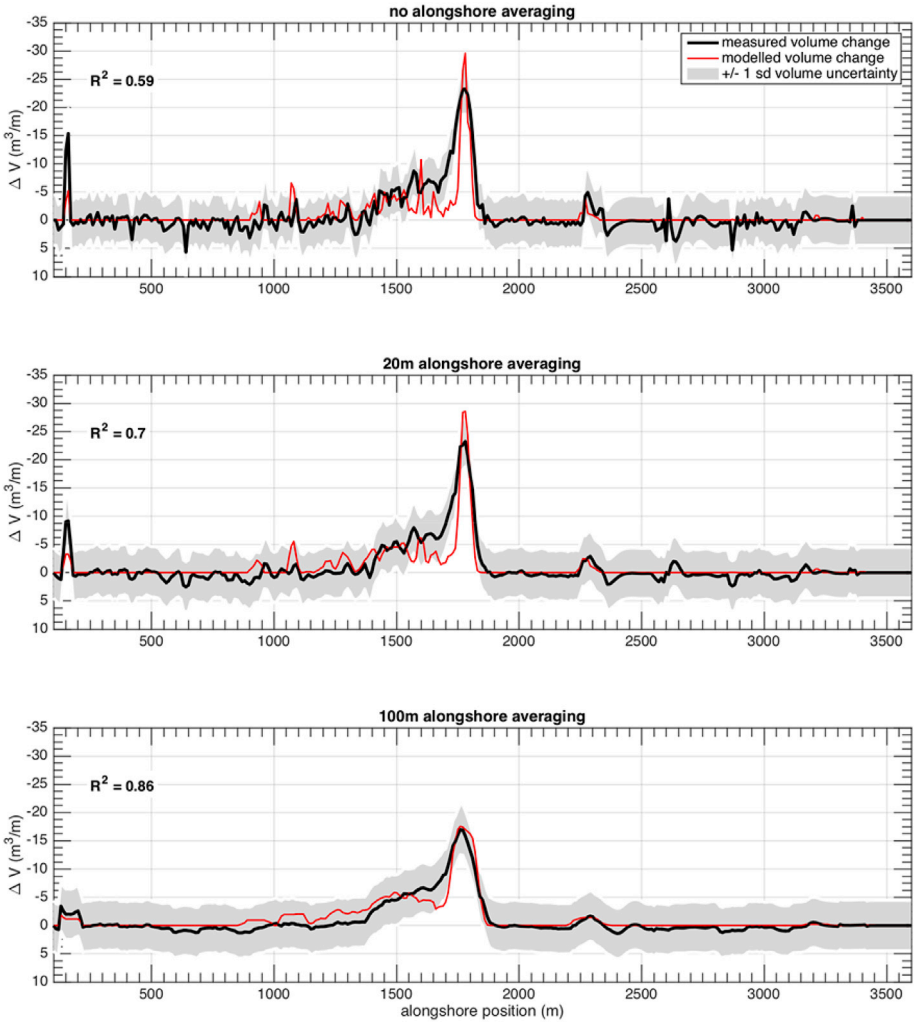

Fig. 9. Comparison of different alongshore averaging lengths on the performance of the simple empirical dune erosion model. (top) No alongshore smoothing. (middle) 20 m alongshore smoothing. (bottom) 100 m alongshore smoothing. Each model was driven with updating topographic data with each lidar survey.

and Palmsten, 2012).

The observations reported here, along with other recent studies of dune erosion in SE Australia (e.g (Splinter and Palmsten, 2012; Palmsten et al., 2014).) where wave runup during storms can reach the dune toe but rarely exceeds the dune crest height, confirm that knowledge of the dune toe elevation is of particular importance at defining the magnitude of erosion within the swash and collision regimes described by Sallenger (2000). For example, in an application of an erosion Bayesian Network to a data set at the Gold Coast in Australia (Palmsten et al., 2014), exclusion of the pre-storm dune toe elevation information resulted in a significant reduction in model skill of more than 50%. In contrast, knowledge of other morphological features is more important in defining erosion magnitude during overwash and inundation (where water levels exceed the dune crest) because different physical processes of dune erosion prevail [e.g (Houser, 2012, 2013; Houser et al., 2008).]. This is confirmed in a second Bayesian Network study (Plant and Stockdon, 2012) that focussed on modelling hurricane response of barrier islands along the east coast of the US (where storm overwash and inundation are commonly observed). In this second study, it was found that variables such as dune height and dune width were more important at predicting dune erosion volumes (Plant and Stockdon, 2012).

5.2. Effect of alongshore averaging

In Fig. 9 the potential impact of alongshore averaging to predictive model performance was examined by applying a moving average window to both the observed and predicted dune erosion volumes, to remove smaller-scale features of alongshore lengths scales *O* (20–100 m). Compared to the unfiltered data (Fig. 9 top), the alongshore averaging had a considerable positive impact on the R^2 values, with greater alongshore spatial averaging (20 m (Fig. 9 middle, $R^2 = 0.70$) vs 100 m (Fig. 9 bottom, $R^2 = 0.86$) increasing the explained variability. Recalling that original modelled wave output was at a 40 m alongshore grid spacing and profiles were extracted every 10 m for the analyses presented here, the physical interpretation for these results lie in the inherent small-scale alongshore variation in beach morphology that is not accounted for in the dune erosion model formulation and smoothed out in the coarser grid wave forcing. By averaging alongshore, this effect is removed and the underlying dune erosion response compared to the smoothed forcing is highlighted. The mathematical reason for the perceived improvement in the model performance comes from the fact that application of a moving average filter reduces the number of independent data points and also removes variability in the two data sets, converging the signal towards linearity and as a result improving an R^2 value. When applying alongshore averaging, the threshold for considering the significance of a model's performance also increases. It is important to note that the smoothed-results still capture the alongshore variable erosion response, which has implications on how much (spatial resolution) data is needed to accurately estimate embayment scale erosion response to storms.

5.3. Offshore versus local wave conditions

At the Narrabeen-Collaroy study site, the availability of a calibrated SWAN model allowed for the estimation of local (nearshore 20 m water depth) wave conditions as detailed in Fig. 3. To determine the increase in model skill that is gained by this knowledge, the model was also forced with the offshore measured deep-water (and hence alongshore uniform) waves as detailed in Fig. 2 (top panel). The model coefficient (C_s) was recalibrated for offshore wave conditions. The model skill dropped by approximately 10%, which is comparable to the decrease in skill between updating profiles daily and using only the pre-storm survey data as discussed in Section 5.1. This suggests that for the simple model formulation used here, alongshore variability in the waves along this 3.6 km embayment explained on the order of 10% of the modelled variance in dune erosion.

5.4. Effect of nearshore morphology

The presence of sandbars or other geological features offshore may impact the overall erosion response during a storm (Stockdon et al., 2007; Harley et al., 2009, 2015; Houser et al., 2008; Schupp et al., 2006). For example, previous studies at Narrabeen-Collaroy have shown that the presence or absence of a sandbar is related to the magnitude of shoreline erosion response (Harley et al., 2009). The lack of a sand bar is correlated to highly accreted beaches and low-energy conditions, far from a storm-energy equilibrium, thus a larger erosion response is expected (Harley et al., 2009, 2015; Davidson et al., 2013). This is in contrast to a beach with a well-developed storm bar that is more in equilibrium with storm conditions, and thus experiences less erosion (Harley et al., 2009, 2015; Davidson et al., 2013). Similarly, the presence of mega-rips (a localized deep channel and lack of bar) have also been show to influence the erosion response of embayed beaches (Loureiro et al., 2012; Thornton et al., 2007).

To better understand the potential influence of nearshore morphology on the observed alongshore-variable erosion response during the June 2011 ECL storm, daily time-exposure ('timex') images captured by an Argus station (Holman et al., 2003) located in the southern end of the embayment are presented (Fig. 10). For reference, the alongshore location where the maximum dune erosion occurred is located between 1000 m < y < 1500 m in the rectified Argus images and indicated by an orange line. Examination of these daily images captured pre, during and immediately post the storm show that pre-storm morphology (June 13th) consisted of a nearshore sandbar with some alongshore variability along the entire beach. Small-scale rip channels and transverse bar - rip channels (identified in the timex images by lack of wave breaking) were present in the middle of the embayment. During the peak of the storm (June 14, 15 16) mega rips are not observed, which if present could potentially have enhanced localized erosion. Post the peak of the storm (June 17–20), small scale rip channels and low-tide terrace bars were observed to develop close to the shoreline in the centre of the embayment, south of the erosion hot-spot, whereas the southern end lacked the presence of an offshore sandbar and the northern end displayed a more alongshore-uniform sandbar. This suggests that while the alongshore variability of the bar may have had some influence on the alongshore variability of the observed erosion response, it is not interpreted to be a key driver.

While the runup formula used in this study does not account explicitly for sandbar morphodynamics in its parameterization (Stockdon et al., 2006), the inclusion of a dry beach slope may serve as a proxy (Harley et al., 2015). Analysing Fig. 6 there is a weak correlation between beach slope and erosion response, but this is not likely a key driver for the alongshore variable beach response observed.

6. Conclusion

Considerable alongshore variability in the observed erosion response to a single storm event along a 3.6 km embayment was captured by daily airborne Lidar surveys over a 6-day period. Pre-storm morphology, such as beach slope, dune toe elevation, and dune height varied considerably alongshore. Using the unique high spatial and temporal resolution 3D surveys of the beach, several key observations were made.

First, at alongshore locations where the pre-storm dune toe was lower, total water levels during the storm exceeded the dune toe and waves collided with the dune resulting in greater dune erosion. Conversely, where dune toes were elevated above the water line and wave runup was predominately limited to the swash regime, very little to no erosion was observed. Considerable alongshore variability in the magnitude of inshore wave heights was not observed to be the primary determinant of localized maximum dune erosion. These observations are consistent with the Storm Impact Scale concept of Sallenger (2000), whereby dune erosion scales with the Total Water Level (sum of ocean water level and 2% runup exceedance) above the elevation of the

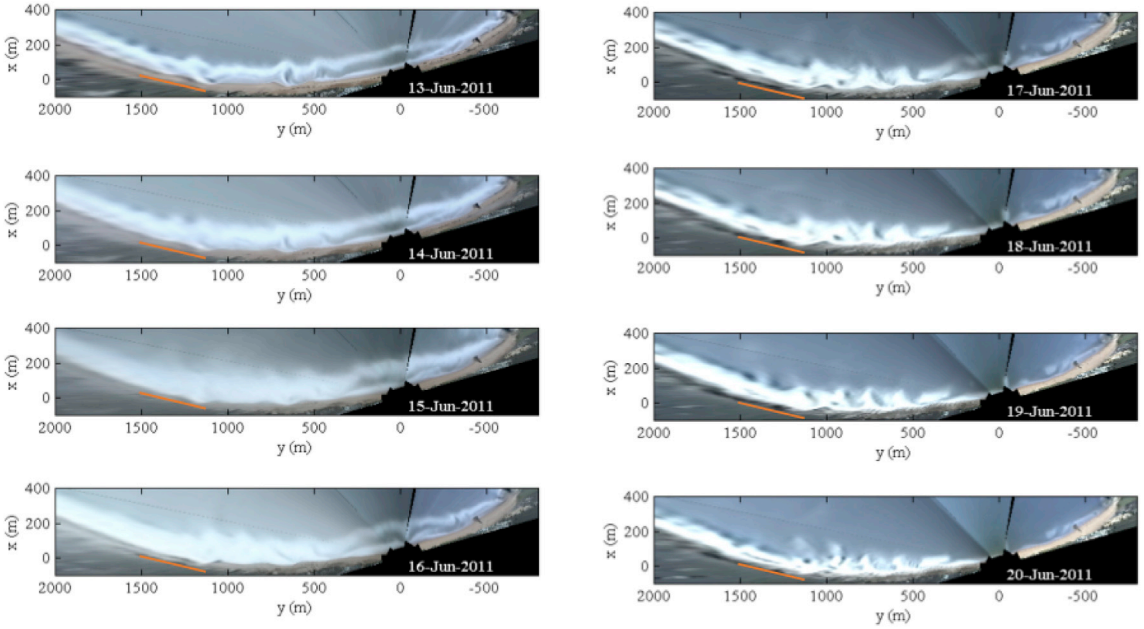

Fig. 10. Daily timex images taken from the Narrabeen-Collaroy Argus station during the storm. Alongshore and Cross-shore axes are in the local Argus coordinate system. The location of the extreme erosion is highlighted by the orange line between 1000 > y > 1500 m. (For interpretation of the references to colour in this figure legend, the reader is referred to the web version of this article.)

pre-storm dune toe.

Second, beach erosion varied through time. While waves were directly colliding with the dune, the dune eroded and the dune toe receded upwards and landwards as the storm progressed. When water levels no longer reached the dune toe, erosion decreased or ceased all together. These field observations are in agreement with lab experiments, such as Palmsten and Holman (2012) and references therein.

Third, at the tail end of the storm, some alongshore locations of the beach were observed to show the initial stages of recovery and sand deposits around the mean water line, highlighting how fast a beach may begin to recover from storm erosion.

From a coastal management and engineering standpoint, a simple dune impact model (Palmsten and Holman, 2012), that estimates dune erosion based on the time-varying total water level relative to the elevation of the dune toe, was able to predict up to 85% of the observed alongshore variability in erosion at this particular site. The modelling confirmed that the temporal variability in observed erosion was tidally modulated over the 6 days and occurred when waves were directly impacting the dune in the 'collision' regime (Sallenger, 2000) at high tide. Importantly, wave modelling indicated that just 10% of the observed alongshore variability in the measured erosion response was likely driven by alongshore variability in the incident wave height on this embayed coastline. The observations and modelling results presented here confirm that knowledge of the pre-storm subaerial profile, in particular the elevation of the dune toe with respect to time-varying water levels during a storm, is a driver of alongshore variability in the erosion response along dune-backed sandy coastlines.

Acknowledgements

The work presented here is part of a Masters by Research (MPhil) thesis by E. Kearney who was funded by an Australian Postgraduate Award. Wave and water level data was provided by the NSW Public Works Manly Hydraulics Laboratory, funded by the NSW Office of Environment and Heritage. Airborne Lidar data was provided by J. Middleton (UNSW School of Aviation). Funding for this work was provided by Australian Research Council Linkage Grant: LP100200348 and by NSW Environmental Trust Environmental Research Program (RD 2015/0128).

Appendix A. Supplementary data

Supplementary data related to this article can be found at https://doi.org/10.1016/j.coastaleng.2017.10.011.

References

Allan, J., Komar, P.D., 2006. Climate controls on US west coast erosion processes. J. Coast. Res. 22, 511–529.

Anderson, T.R., Fletcher, C.H., Barbee, M.M., Frazer, L.N., Romine, B.M., 2015. Doubling of coastal erosion under rising sea level by mid-century in Hawaii. Nat. Hazards 75–103. https://doi.org/10.1007/s11069-015-1698-6.

Aubrey, D.G., 1979. Seasonal patterns of onshore/offshore sediment movement. J. Geophys. Res. 84, 6347–6354.

Barnard, P.L., Allan, J., Hansen, J.E., Kaminsky, G.M., Ruggiero, P., Doria, A., 2011. The impact of the 2009-10 El niño Modoki on U.S. West coast beaches. Geophys. Res. Lett. 38, L13604. https://doi.org/10.1029/2011GL047707.

Barnard, P.L., Short, A.D., Harley, M.D., Splinter, K.D., Vitousek, S., Turner, I.L., Allan, J., Banno, M., Bryan, K.R., Doria, A., Hansen, J.E., Kato, S., Kuriyama, Y., Randall-Goodwin, E., Ruggiero, P., Walker, I.J., Heathfield, D.K., 2015. Coastal vulnerability across the Pacific dominated by El niño/southern oscillation. Nat. Geosci. 1–8. https://doi.org/10.1038/ngeo2539.

Booij, N., Ris, R.C., Holthuijsen, L.H., 1999. A third-generation wave model for coastal regions 1. Model description and validation. J. Geophys. Res. Ocean. 104, 7649–7666.

Bryant, E., Kidd, R., 1975. Beach erosion, may-june, 1974, central and south coast, NSW. Search 6, 511–513.

Callaghan, D.P., Roshanka, R., Andrew, S., Ranasinghe, R., Short, A.D., 2009. Quantifying the storm erosion hazard for coastal planning. Coast. Eng. 56, 90–93. https://doi.org/10.1016/j.coastaleng.2008.10.003.

Callaghan, D.P., Ranasinghe, R., Roelvink, D., 2013. Probabilistic estimation of storm erosion using analytical, semi-empirical, and process based storm erosion models. Coast. Eng. 82, 64–75. https://doi.org/10.1016/j.coastaleng.2013.08.007.

Castelle, B., Marieu, V., Bujan, S., Splinter, K.D., Robinet, A., Sénéchal, N., Ferreira, S., 2015. Impact of the winter 2013-2014 series of severe Western Europe storms on a double-barred sandy coast: beach and dune erosion and megacusp embayments. Geomorphology. https://doi.org/10.1016/j.geomorph.2015.03.006.

Coco, G., Senechal, N., Rejas, A., Bryan, K.R., Capo, S., Parisot, J.P., Brown, J. a., MacMahan, J.H.M., 2014. Beach response to a sequence of extreme storms. Geomorphology 204, 493–501. https://doi.org/10.1016/j.geomorph.2013.08.028.

Davidson, M.A., Splinter, K.D., Turner, I.L., 2013. A simple equilibrium model for predicting shoreline change. Coast. Eng. 73, 191–202. https://doi.org/10.1016/j.coastaleng.2012.11.002.

Foster, D.G., Gordon, A.D., Lawson, N.V., 1975. The storms of may-june 1974, Sydney,NSW. In: 2nd Aust. Conf. Coast. Ocean Eng. The Institution of Engineers, Australia, pp. 1–11.

Frazer, L.N., Anderson, T.R., Fletcher, C.H., 2009. Modeling storms improves estimates of long-term shoreline change. Geophys. Res. Lett. 36, L20404. https://doi.org/10.1029/2009GL040061.

Harley, M.D., Turner, I.L., 2008. A simple data transformation technique for pre-processing survey data at embayed beaches. Coast. Eng. 55, 63–68. https://doi.org/10.1016/j.coastaleng.2007.07.001.
Harley, M.D., Turner, I.L., Short, A.D., Ranasinghe, R., 2009. An empirical model of beach response to storms - SE Australia. Coasts Ports 2009 a Dyn. Environ. 600–606.
Harley, M.D., Turner, I.L., Short, A.D., Ranasinghe, R., 2011. A re-evaluation of coastal embayment rotation: the dominance of cross-shore versus alongshore sediment transport processes, Collaroy-Narrabeen Beach, SE Australia. J. Geophys. Res. 116, F04033. https://doi.org/10.1029/2011JF001989.
Harley, M.D., Turner, I.L., Short, A.D., 2015. New insights into embayed beach rotation: the importance of wave exposure and cross-shore processes. J. Geophys. Res. F. Earth Surf. 120, 1470–1484. https://doi.org/10.1002/2014JF003390.
Harley, M.D., Valentini, A., Armaroli, C., Perini, L., Calabrese, L., Ciavola, P., 2016. Can an early-warning system help minimize the impacts of coastal storms? A case study of the 2012 Halloween storm, northern Italy. Nat. Hazards Earth Syst. Sci. 16, 209–222. https://doi.org/10.5194/nhess-16-209-2016.
Harley, M.D., Turner, I.L., Kinsela, M.A., Middleton, J.H., Mumford, P.J., Splinter, K.D., Phillips, M.S., Simmons, J.A., Hanslow, D.J., Short, A.D., 2017. Extreme coastal erosion enhanced by anomalous extratropical storm wave direction. Sci. Rep. 7, 6033. https://doi.org/10.1038/s41598-017-05792-1.
Holman, R., Stanley, J., Özkan-Haller, T., 2003. Applying video sensor networks to nearshore environment monitoring. IEEE Pervasive Comput. 2, 14–21. https://doi.org/10.1109/MPRV.2003.1251165.
Houser, C., 2012. Feedback between ridge and swale bathymetry and barrier island storm response and transgression. Geomorphology 173–174, 1–16. https://doi.org/10.1016/j.geomorph.2012.05.021.
Houser, C., 2013. Alongshore variation in the morphology of coastal dunes: implications for storm response. Geomorphology 199, 48–61. https://doi.org/10.1016/j.geomorph.2012.10.035.
Houser, C., Hapke, C., Hamilton, S., 2008. Controls on coastal dune morphology, shoreline erosion and barrier island response to extreme storms. Geomorphology 100, 223–240. https://doi.org/10.1016/j.geomorph.2007.12.007.
IPCC, Nicholls, R.J., Wong, P.P., Burkett, V.R., Codignotto, J.O., Hay, J.E., McLean, R.F., Ragoonaden, S., Woodroffe, C.D., 2007. Contribution of Working Group II to the Fourth Assessment Report of the Intergovernmental Panel on Climate Change. Cambridge University Press, Cambridge, UK.
Larson, M., Erikson, L., Hanson, H., 2004. An analytical model to predict dune erosion due to wave impact. Coast. Eng. 51, 675–696. https://doi.org/10.1016/j.coastaleng.2004.07.003.
Loureiro, C., Ferreira, Ó., Cooper, J.A.G., 2012. Extreme erosion on high-energy embayed beaches: influence of megarips and storm grouping. Geomorphology 139–140, 155–171. https://doi.org/10.1016/j.geomorph.2011.10.013.
Mariani, A., Shand, T.D., Carley, J.T., Goodwin, I.D., Splinter, K., Davey, E.K., Flocard, F., Turner, I.L., 2012. Generic Design Coastal Erosion Volumes and Setbacks for Australia. Research Report 247. Australia, Sydney. https://doi.org/10.4225/53/5786faf5b3c5c.
Masselink, G., Castelle, B., Scott, T., Dodet, G., Suanez, S., Jackson, D., Floc, F., 2016. Extreme wave activity during 2013/2014 winter and morphological impacts along the Atlantic coast of Europe. Geophys. Res. Lett. 43, 2135–2143. https://doi.org/10.1002/2015GL067492.Received.
Masselink, G., Scott, T., Poate, T., Russell, P., Davidson, M., Conley, D., 2016. The extreme 2013/2014 winter storms: hydrodynamic forcing and coastal response along the southwest coast of England. Earth Surf. Process. Landforms 41, 378–391. https://doi.org/10.1002/esp.3836.
McCall, R.T., Van Thiel de Vries, J.S.M., Plant, N.G., Van Dongeren, A.R., Roelvink, J.A., Thompson, D.M., Reniers, A.J.H.M., 2010. Two-dimensional time dependent hurricane overwash and erosion modeling at Santa Rosa Island. Coast. En. 57, 668–683.
McGrath, B.L., 1968. Erosion of Gold coast beaches. J. Inst. Eng. Aust. 40, 155–166.
McLean, R.F., Thom, B.G., 1975. Beach changes at Moruya, 1972-74. In: Coast. Ocean Eng. Engineers Australia, National Conference Publication No. 75/2, pp. 12–17.
Middleton, J.H., Cooke, C.G., Kearney, E.T., Mumford, P.J., Mole, M.A., Nippard, G.J., Rizos, C., Splinter, K.D., Turner, I.L., 2013. Resolution and accuracy of an airborne scanning laser system for beach surveys. J. Atmos. Ocean. Technol. 30, 2452–2464. https://doi.org/10.1175/JTECH-D-12-00174.1.
Morton, R.A., Leach, M.P., Paine, J.G., Cardoza, M.A., 1993. Monitoring beach changes using Gps surveying techniques. J. Coast. Res. 9, 702–720.
Mull, J., Ruggiero, P., 2014. Estimating storm-induced dune erosion and overtopping along U.S. West coast beaches. J. Coast. Res. 298, 1173–1187. https://doi.org/10.2112/JCOASTRES-D-13-00178.1.
Overton, M.F., Fisher, J.S., 1988. Simulation modeling of dune erosion. In: Edge, B.L. (Ed.), 21st Int. Conf. Coast. Eng. ASCE, Costa del Sol-Malaga, Spain, pp. 1857–1867.
Overton, M.F., Fisher, J.S., Hwang, K.N., 1994. Development of a dune erosion model using SUPERTANK data. In: Edge, B.L. (Ed.), 24th Int. Conf. Coast. Eng. ASCE, Kobe, Japan, pp. 2488–2502.
Palmsten, M.L., Holman, R.A., 2012. Laboratory investigation of dune erosion using stereo video. Coast. Eng. 60, 123–135.
Palmsten, M.L., Splinter, K.D., 2016. Observations and simulations of wave runup during a laboratory dune erosion experiment. Coast. Eng. 115, 58–66. https://doi.org/10.1016/j.coastaleng.2016.01.007.
Palmsten, M.L., Splinter, K.D., Plant, N.G., Stockdon, H.F., 2014. Probabilistic estimation of dune retreat on the Gold Coast, Australia. Shore Beach 82, 35–43.
Plant, N.G., Stockdon, H.F., 2012. Probabilistic prediction of barrier-island response to hurricanes. J. Geophys. Res. Earth Surf. 117, 1–17. https://doi.org/10.1029/2011JF002326.
Pye, K., Blott, S.J., 2008. Decadal-scale variation in dune erosion and accretion rates: an investigation of the significance of changing storm tide frequency and magnitude on the Sefton coast, UK. Geomorphology 102, 652–666. https://doi.org/10.1016/j.geomorph.2008.06.011.
Quartel, S., Kroon, A., Ruessink, B.G., 2008. Seasonal accretion and erosion patterns of a microtidal sandy beach. Mar. Geol. 250, 19–33. https://doi.org/10.1016/j.margeo.2007.11.003.
Ranasinghe, R., Callaghan, D.P., Roelvink, D., 2013. Does a more sophisticated storm erosion model improve probabilistic erosion estimates?. In: 7th Inernational Conf. Coast. Dyn, pp. 1277–1286.
Roelvink, D., Reniers, A., van Dongeren, A., van Thiel de Vries, J., McCall, R., Lescinski, J., 2009. Modelling storm impacts on beaches, dunes and barrier islands. Coast. Eng. 56, 1133–1152. https://doi.org/10.1016/j.coastaleng.2009.08.006.
Ruggiero, P., Kaminsky, G.M., Hacker, S., 2013. Morphodynamics of Prograding beaches. Coast. Dyn. 1375–1384.
Russell, P.E., 1993. Mechanisms for beach erosion during storms. Cont. Shelf Res. 13, 1243–1265.
Sallenger, A.H.J., 2000. Storm impact scale for barrier islands. J. Coast. Res. 16, 890–895.
Saye, S.E., van der Wal, D., Pye, K., Blott, S.J., 2005. Beach-dune morphological relationships and erosion/accretion: an investigation at five sites in England and Wales using LIDAR data. Geomorphology 72, 128–155. https://doi.org/10.1016/j.geomorph.2005.05.007.
Schupp, C.A., McNinch, J.E., List, J.H., 2006. Nearshore shore-oblique bars, gravel outcrops, and their correlation to shoreline change. Mar. Geol. 233, 63–79.
Senechal, N., Coco, G., Castelle, B., Marieu, V., 2015. Storm impact on the seasonal shoreline dynamics of a meso- to macrotidal open sandy beach (Biscarrosse, France). Geomorphology 228, 448–461. https://doi.org/10.1016/j.geomorph.2014.09.025.
Serafin, K.A., Ruggiero, P., 2014. Simulating extreme total water levels using a time-dependent, extreme value approach. J. Geophys. Res. Ocean. 119, 6305–6329. https://doi.org/10.1002/2014JC010093.Received.
Shand, T.D., Goodwin, I.D., Mole, M.A., Carley, J.T., Browning, S., Coghlan, I.R., Harley, M.D., Peirson, W.L., 2011. NSW Coastal Inundation Hazard Study: Coastal Storms and Extreme Waves.
Simmons, J.A., Harley, M.D., Marshall, L.A., Turner, I.L., Splinter, K.D., Cox, R.J., 2017. Calibrating and assessing uncertainty in coastal numerical models. Submitt. Coast. Eng 125, 28–41. https://doi.org/10.1016/j.coastaleng.2017.04.005.
Splinter, K.D., Palmsten, M.L., 2012. Modeling dune response to an East coast low. Mar. Geol. 329–331, 46–57. https://doi.org/10.1016/j.margeo.2012.09.005.
Splinter, K.D., Carley, J.T., Golshani, A., Tomlinson, R., 2014. A relationship to describe the cumulative impact of storm clusters on beach erosion. Coast. Eng. 83, 49–55. https://doi.org/10.1016/j.coastaleng.2013.10.001.
Stive, M.J.F., Aarninkhof, S.G.J., Hamm, L., Hanson, H., Larson, M., Wijnberg, K.M., Nicholls, R.J., Capobianco, M., 2002. Variability of shore and shoreline evolution. Coast. Eng. 47, 211–235. https://doi.org/10.1016/S0378-3839(02)00126-6.
Stockdon, H.F., Holman, R.A., Howd, P.A., Sallenger, A.H., 2006. Empirical parameterization of setup, swash, and runup. Coast. Eng. 53, 573–588. https://doi.org/10.1016/j.coastaleng.2005.12.005.
Stockdon, H.F., Sallenger Jr., A.H., Holman, R.A., Howd, P.A., 2007. A simple model for the spatially-variable coastal response to hurricanes. Mar. Geol. 238, 1–20. https://doi.org/10.1016/j.margeo.2006.11.004.
Stockdon, H.F., Doran, K.S., Sallenger, A.H., 2009. Extraction of lidar-based dune-crest elevations for use in examining the vulnerability of beaches to inundation during hurricanes. J. Coast. Res. 59–65. https://doi.org/10.2112/SI53-007.1.
Thornton, E.B., MacMahan, J., Sallenger, A.H., 2007. Rip currents, mega-cusps, and eroding dunes. Mar. Geol. 240, 151–167. https://doi.org/10.1016/j.margeo.2007.02.018.
Turner, I.L., Harley, M.D., Short, A.D., Simmons, J.A., Bracs, M.A., Phillips, M.S., Splinter, K.D., 2016. A multi-decade dataset of monthly beach profile surveys and inshore wave forcing at Narrabeen, Australia. Sci. Data 3, 160024. https://doi.org/10.1038/sdata.2016.24.
van Verseveld, H.C.W., van Dongeren, A.R., Plant, N.G., Jäger, W.S., den Heijer, C., 2015. Modelling multi-hazard hurricane damages on an urbanized coast with a Bayesian Network approach. Coast. Eng. 103, 1–14. https://doi.org/10.1016/j.coastaleng.2015.05.006.
Vousdoukas, M.I., Ferreira, Ó., 2012. Toward reliable storm-hazard forecasts: XBeach calibration and its potential application in an operational early-warning system. Ocean Dynamics 62, 1001–1015. https://doi.org/10.1007/s10236-012-0544-6.
Wright, L.D., Short, A.D., 1984. Morphodynamic variability of surf zones and beaches: a synthesis. Mar. Geol. 56, 93–118. https://doi.org/10.1016/0025-3227(84)90008-2.